

REPORT DOCUMENTATION PAGE

Form Approved
OMB No. 0704-0188

Public reporting burden for this collection of information is estimated to average 1 hour per response, including the time for reviewing instructions, searching existing data sources, gathering and maintaining the data needed, and completing and reviewing this collection of information. Send comments regarding this burden estimate or any other aspect of this collection of information, including suggestions for reducing this burden to Department of Defense, Washington Headquarters Services, Directorate for Information Operations and Reports (0704-0188), 1215 Jefferson Davis Highway, Suite 1204, Arlington, VA 22202-4302. Respondents should be aware that notwithstanding any other provision of law, no person shall be subject to any penalty for failing to comply with a collection of information if it does not display a currently valid OMB control number. PLEASE DO NOT RETURN YOUR FORM TO THE ABOVE ADDRESS.

1. REPORT DATE (DD-MM-YYYY) 05-21-04		2. REPORT TYPE Technical Paper		3. DATES COVERED (From - To)	
4. TITLE AND SUBTITLE A Photoelastic Study of Cracking in Motor Grain Models				5a. CONTRACT NUMBER	
				5b. GRANT NUMBER	
				5c. PROGRAM ELEMENT NUMBER	
6. AUTHOR(S) C.W. Smith, J.D. Hansen				5d. PROJECT NUMBER 2302	
				5e. TASK NUMBER 0378	
				5f. WORK UNIT NUMBER 23020378	
7. PERFORMING ORGANIZATION NAME(S) AND ADDRESS(ES) Air Force Research Laboratory (AFMC) AFRL/PRS 5 Pollux Drive Edwards AFB, CA 93524-7048				8. PERFORMING ORGANIZATION REPORT NUMBER	
9. SPONSORING / MONITORING AGENCY NAME(S) AND ADDRESS(ES) Air Force Research Laboratory (AFMC) AFRL/PRS 5 Pollux Drive Edwards AFB, CA 93524-7048				10. SPONSOR/MONITOR'S ACRONYM(S)	
				11. SPONSOR/MONITOR'S NUMBER(S) AFRL-PR-ED-VG-2004-178	
12. DISTRIBUTION / AVAILABILITY STATEMENT Approved for public release; distribution unlimited.					
13. SUPPLEMENTARY NOTES SEM X International Congress & Exposition on Experimental And Applied Mechanics Costa Mesa, CA. 7-10 Jun 2004					
14. ABSTRACT					
20040715 193					
15. SUBJECT TERMS					
16. SECURITY CLASSIFICATION OF:			17. LIMITATION OF ABSTRACT	18. NUMBER OF PAGES	19a. NAME OF RESPONSIBLE PERSON
					Linda Talon
a. REPORT	b. ABSTRACT	c. THIS PAGE			19b. TELEPHONE NUMBER (include area code)
Unclassified	Unclassified	Unclassified	A	10	(661) 275-5283

Standard Form 298 (Rev. 8-98)
Prescribed by ANSI Std. Z39.18

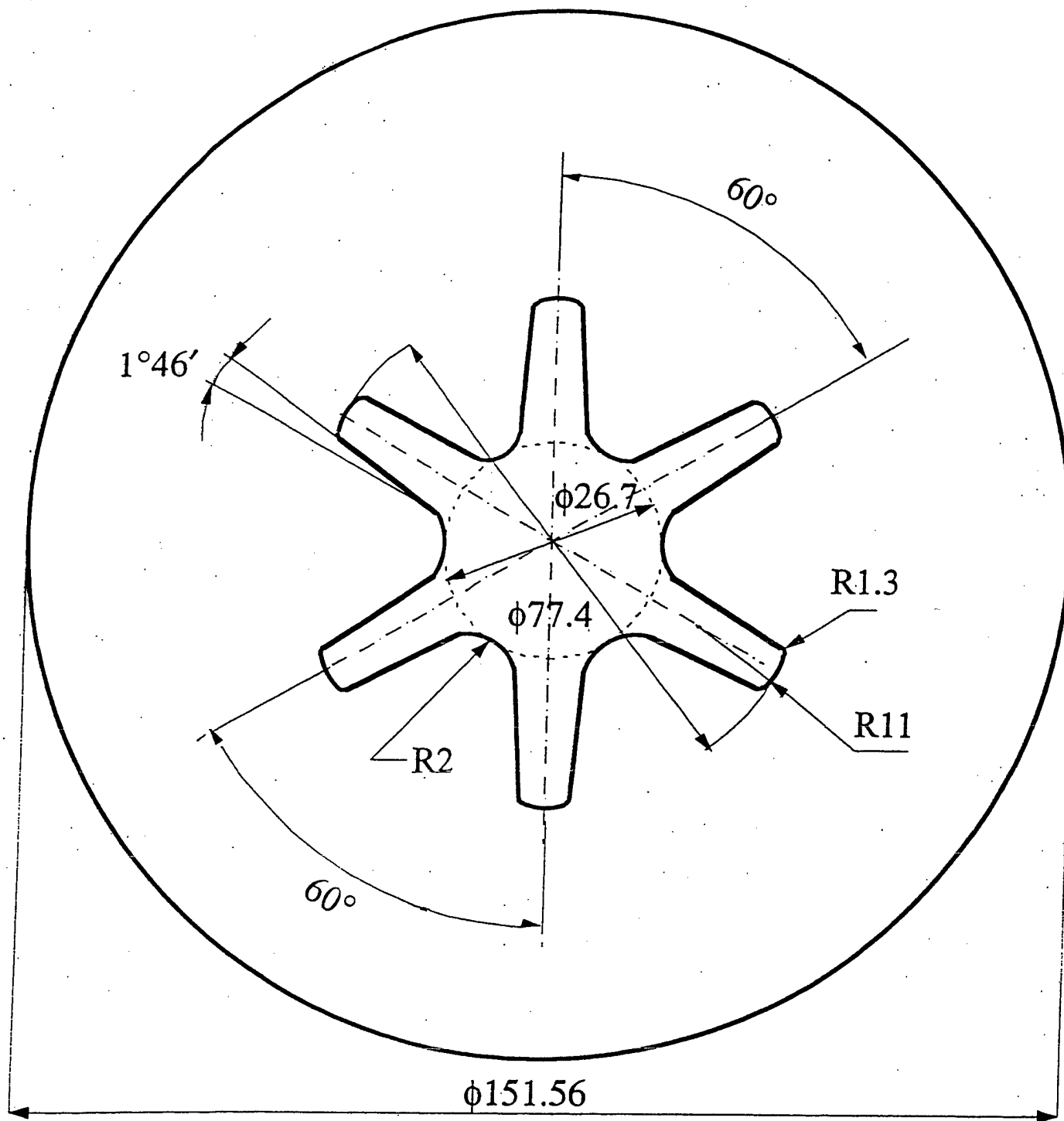
BEST AVAILABLE COPY

A PHOTOELASTIC STUDY OF CRACKING IN MOTOR GRAIN MODELS

C. W. Smith and J. D. Hansen

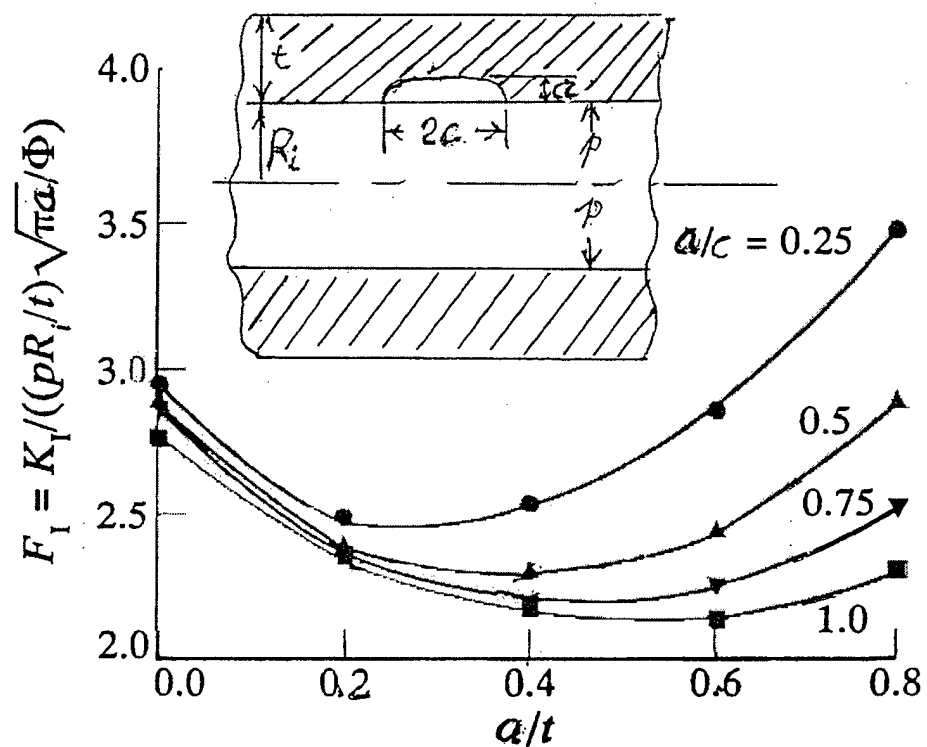
Department of Engineering Science and Mechanics
Virginia Polytechnic Institute and State University
Blacksburg, Virginia 24061-0219

length of cylinder 376 mm



all dimensions are in mm

Figure 2: Crosssection of test models.



(b) $t/R_i = 1.0$

- Results from BEM showing "dish" shaped region for normalized SIF for a semi-elliptical surface crack in a pressurized thick walled cylinder.
- $F_I - K_I$ = SIF; p = pressure, Φ = Elliptic Integral of Second Kind. See Table 1 slide.

Model 3

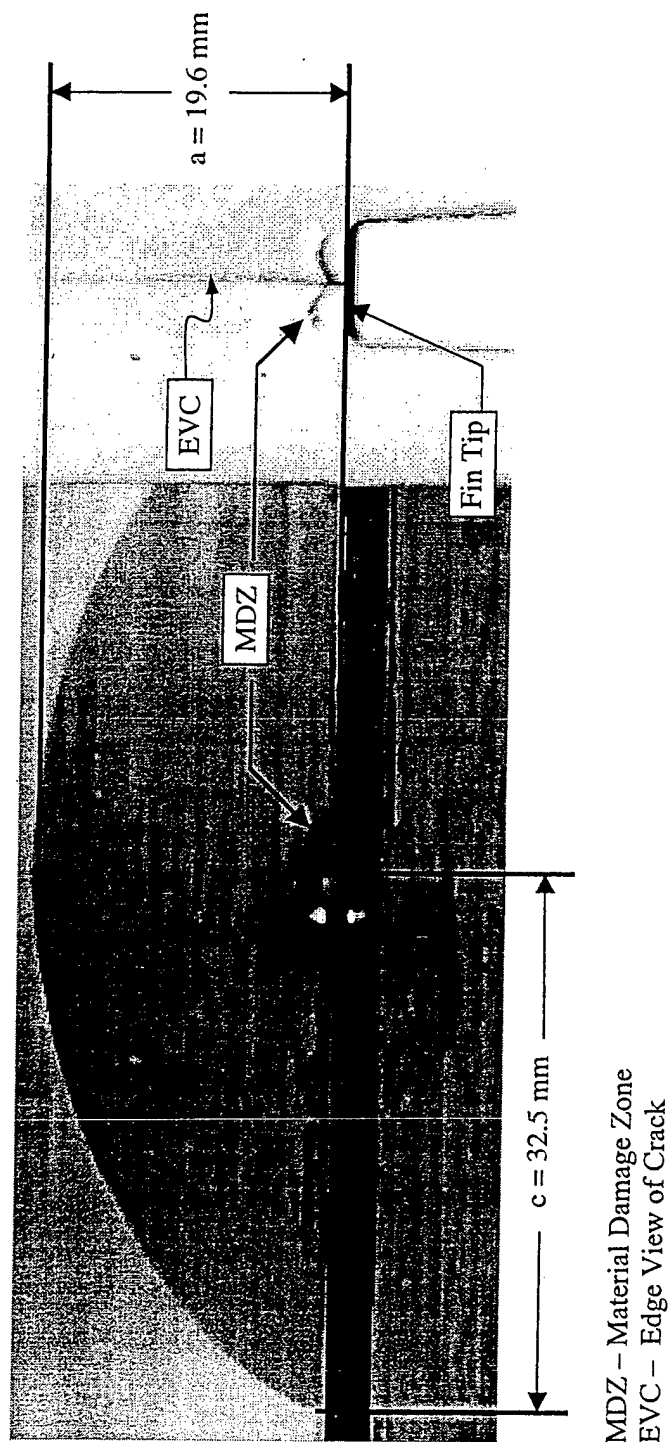
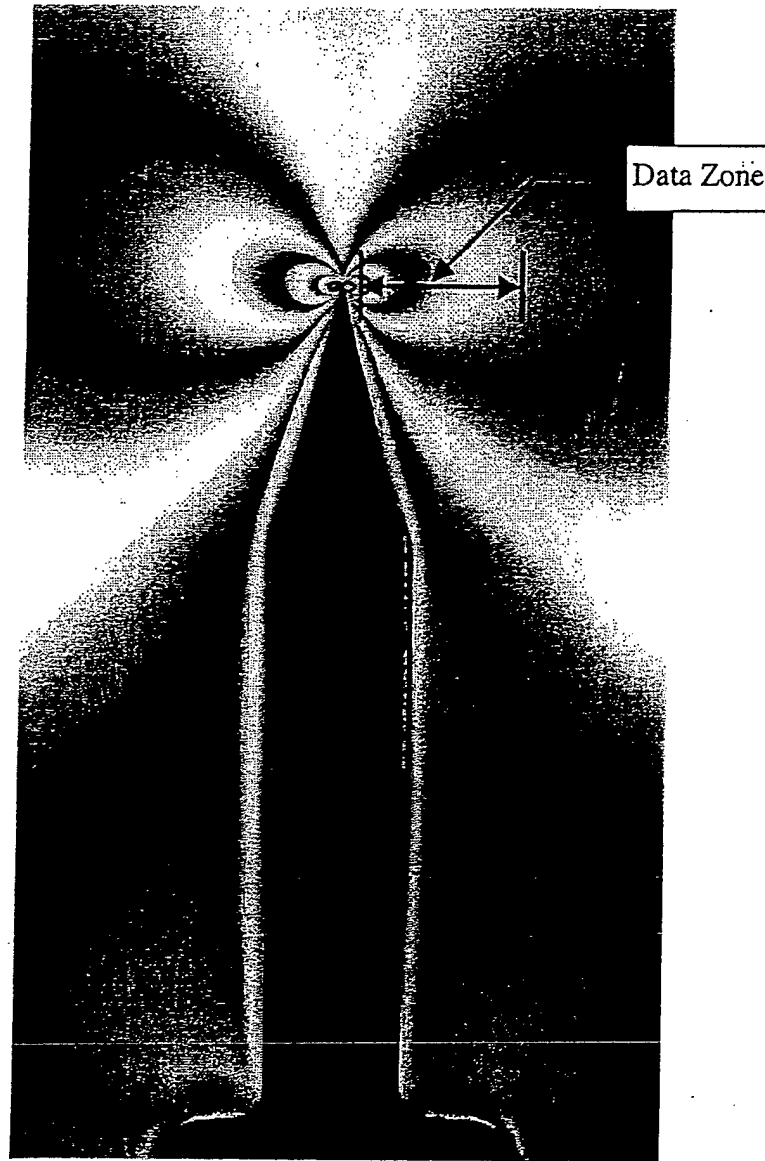


Figure 3: Crack shape and fin tip location for model 3

57

Model 6b

Center Slice ($t = 4.29$ mm)



P_{sf} : 2.3×10^{-2} MPa

c_f : 175.30 mm

a_f : 19.6 mm

Data zone: $(r_{ave})_2 - (r_{ave})_1 = 4.2635 - 0.4564 = 3.807$ mm

Figure 4: Unmultiplied fringe pattern from a 4.3mm slice from the center of the crack for Model 6 using a diffused light polariscope for a machined crack denoting location of data zone.

Mode I Algorithm For Determination of Stress Intensity Factor (SIF)

In linear elastic fracture mechanics (LEFM) using the photoelastic approach, one can begin with Mode I near tip equations (Fig. A-1)

$$\sigma_{ij} = \frac{K_I}{\sqrt{8\pi r}} f_{ij}(\theta) + \sigma_{ij}^o \quad (i,j = n, z) \quad (A-1)$$

where K_I is the Mode I SIF, σ_{ij}^o are the contribution of the nonsingular stresses in the measurement zone, and r, θ then are centered at the crack tip. The following expression is computed, in truncated form, along $\theta = \pi/2$, where fringe spreading is greatest. (Fig. A-2) Thus

$$\tau_{max}^{nz} = \frac{K_{AP}}{\sqrt{8\pi r}} = \frac{K_I}{\sqrt{8\pi r}} + \tau_0 \quad (A-2)$$

where K_{AP} is an "apparent" SIF, which includes the effect of σ_{ij}^o {i.e., $\tau_0 = f(\sigma_{ij}^o)$ } with the singular effect in the measurement zone. The stress-optic law states that $\tau_{max}^{nz} = \frac{N_I}{2t}$, where N is the measured stress fringe order, f is the material fringe value and t the slice thickness. Thus τ_{max}^{nz} is proportional to N and may be regarded as the measured quantity together with r . By rearranging terms in Eq. A-2 and normalizing, we can obtain

$$\frac{K_{AP}\Phi}{p\sqrt{\pi a}} = \frac{K_I\Phi}{p\sqrt{\pi a}} + \frac{\sqrt{8}}{p}\pi_o\Phi\left(\sqrt{\frac{r}{a}}\right) \quad (A-3)$$

for a semi-elliptic crack where the coefficient of $\sqrt{r/a}$ is a constant, p is the internal pressure and a is the crack size. Φ is an elliptic integral which varies with the aspect ratio of the crack (a/c). Its form is approximated by \sqrt{Q} where Q is given in Table I. In general, when applied to cylindrical vessels, the denominator of Eq. A-3 should be $p\frac{R_i}{t}$. However, in the present problem geometry, $R_i/t = 1$, and the R_i/t can be dropped here.

By defining the normalized SIF as

$$F = \frac{K_{AP}\sqrt{Q}}{p\sqrt{\pi a}} \quad (A-4)$$

one can plot F vs. $\sqrt{r/a}$ and locate the linear zone implied by Eq. A-3, which is the zone dominated by the stress singularity. By extending this line to the origin, the value of F is determined as shown in Fig. A.3 for Model 1.

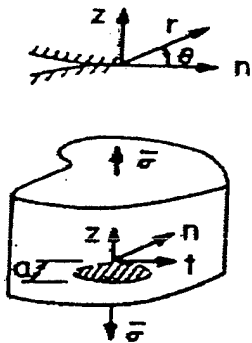


Fig. A-1: Mode I Near Tip Notation

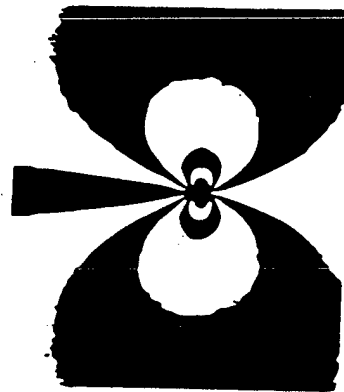


Fig. A-2: Mode I Fringe (Pattern Unmultiplied)

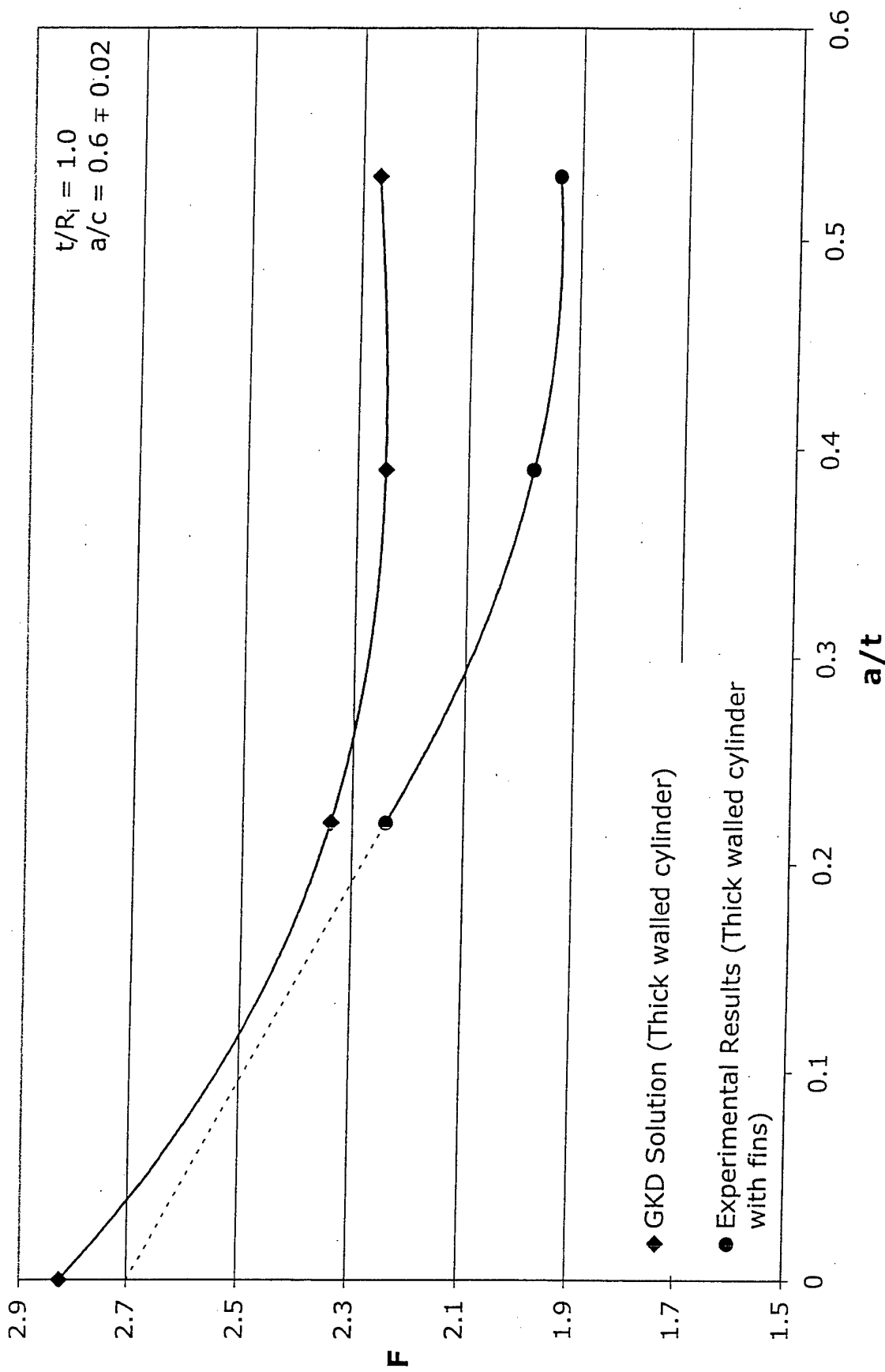


Figure 5: Comparison of experimental results for part through cracks in star finned models with same depth cracks in the pressurized cylinder models (GKD) in the central "dish bottom" region.

Model #1 Center, Normalized

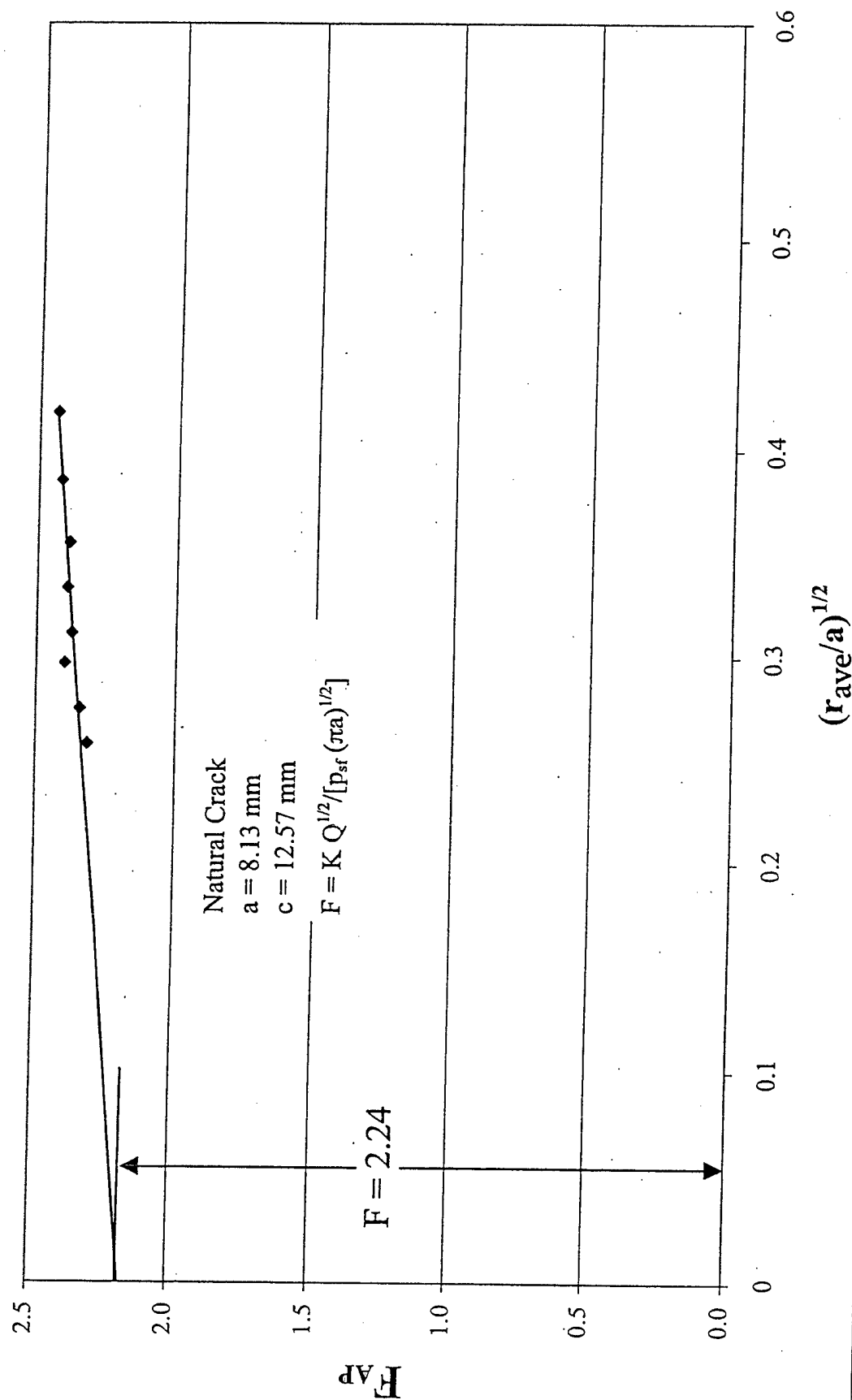


Figure A-3: Determination of Normalized Stress Intensity Factor (F) from Test Data.

Table 1
Test Data and Computed Results

Col	1	2	3	4	5	6	7	8	9	10	11	12	13	14
Test	a	c	a/c	a/t	ρ_{sf}	ρ_{max}	K_{EXP}	K_{GKD}	K_{BF}	K_{PSE}	F_{GKD}	F_{BF}	F_{EXP}	F_{PSE}
1	8.13	12.57	0.65	0.22	0.041	0.121	0.35	0.37	0.57	0.55	2.34	2.77	2.24	2.65
2	14.6	23.00	0.63	0.39	0.046	0.129	0.47	0.54	0.93	0.82	2.25	2.99	1.98	2.63
3*	19.6	32.50	0.60	0.53	0.028	0.167	0.33	0.39	0.70	0.60	2.27	3.17	1.94	2.71
4	8.31	183.24	0.05	0.22	0.041	0.041	0.46	0.56	0.58	0.48	2.70	2.77	2.22 ⁺	2.28
5	14.6	181.65	0.08	0.39	0.041	0.041	0.68	0.73	0.83	0.78	2.65	2.99	2.49 ⁺	2.81
6	19.6	175.30	0.11	0.53	0.023	0.023	0.44	0.48	0.57	0.52	2.70	3.17	2.47 ⁺	2.90

Linear dimensions -mm

Pressure = N/mm^2

K values = $\frac{N}{mm^{3/2}}$

ρ_{sf} = Stress freezing pressure t = Cylinder wall thickness or (distance from fin tip to outer boundary)
subscript notations

KGD = Gouzhong, Kangda and Dongdi (For Cyl.)

BF = Bowie & Freese (for Cyl.)

$$K_{PSE} = K_{EXP} \left(\frac{K_{BF}}{K_{GKD}} \right)$$

⁺ These crack shapes were not semi-elliptical or through the length cracks.

* Cylinder length was 336mm

$$F = \frac{K_1 \sqrt{Q}}{p R_i / t \sqrt{\pi a}} : \sqrt{Q} = \phi = \text{elliptic Integral of 2nd kind}$$

$$R_i = \text{Inner cylinder radius } Q \approx 1 + 1.464 \left(\frac{a}{c} \right)^{1.65} \frac{a}{c} < 1$$

Summary

By capitalizing on observed similarities between the cracked finned model and a cracked cylinder when placing the fin tip at the inner edge of the cylinder, estimates were made by assuming a plane strain solution for the finned model in finite length models. Based upon the aforementioned limited results, use of a modified plane strain solution appears to yield a slightly conservative prediction for long shallow cracks to significantly conservative prediction for deep part-through cracks.